Influence of Polymer Blending of Cellulose Acetate Butyrate for CO_2/N_2 Separation

Shi Chin Ng,[1] Zeinab Abbas Jawad,[1*] Peng Chee Tan,[2] Bridgid Lai Fui Chin[1] and Ren Jie Lee[1]

[1]Department of Chemical Engineering, Faculty of Engineering and Science, Curtin University Malaysia, 98009 Sarawak, Malaysia
[2]School of Energy and Chemical Engineering, Xiamen University Malaysia, Jalan Sunsuria, Bandar Sunsuria, 43900 Sepang, Selangor, Malaysia

*Corresponding author: zeinab.aj@curtin.edu.my

ABSTRACT: *In recent years, carbon dioxide (CO_2) emission has increased significantly. To overcome this issue, carbon capture and storage was implemented to remove CO_2 due to its low energy consumption and economic advantages. As a result, membrane technology was introduced as one of the technologies for CO_2 separation to capture CO_2 from industrial processes. Cellulose acetate butyrate (CAB) was selected as the material for polymeric membrane due to its high CO_2 solubility. The CAB membrane was fabricated by blending two CAB polymers at different molecular weights of 70000 and 65000 using the wet-phase inversion method. A study of the parameter was carried out as it affected the structure and separation performance of the membrane in particular, polymer concentration. The results showed the satisfactory performance of CAB membrane blended with molecular weights of 70000 and 65000 at a ratio of 40:60 (M3) where, the CO_2 permeance, nitrogen (N_2) permeance and CO_2/N_2 selectivity were 26.39 GPU, 7.73 GPU and 3.41 GPU, respectively. Hence, it is expected that this research may apply to membrane gas separation in industries such as power plants to separate CO_2 from exhaust gas and reduce CO_2 emissions.*

Keywords: Cellulose acetate butyrate, gas separation, polymer concentration, polymer blending, membrane separation

1. INTRODUCTION

In the 21st century, the carbon dioxide (CO_2) concentration in the atmosphere has increased considerably. CO_2 has been classified as the primary anthropogenic greenhouse gas. Further, the sources of CO_2 emission have been found from combustion of fossil fuels and industrial processes.[1]

Amongst all the CO_2 separation technologies, membrane separation is a feasible carbon capture and storage technology for removal of CO_2. Therefore, membrane technology has become attractive to industries as it is environmentally friendly, easy to scale up and energy efficient.[2] Hence, there are many types of polymers such as cellulose ester, cellulose nitrate, cellulose propionate, methylcellulose, ethyl cellulose, hydroxypropyl methyl cellulose, fluorinated cellulose acetate and cellulose acetate butyrate (CAB).[3] Among these polymers, CAB was selected as the polymer material for membrane due to its outstanding characteristics of great film forming properties, and better thermal and chemical stability compared with cellulose acetate materials, which have a bulky functional group.[4] In addition, the butyryl and acetyl groups within the CAB polymer enlarges the capacity of the cellulose chain membrane causing high CO_2 solubility in CAB.[5] However, there is a limitation of the polymeric membrane, which affects the separation performance of the membrane. This limitation is the trade-off relationship between gas permeability and selectivity, whereby a polymer with high selectivity has low permeability and vice versa.[6]

To overcome this issue, one of the methods to enhance the separation performance of the polymeric membrane is polymeric blending. According to Mukhtar et al., the polysulfone/polyetherimide (PSF/PEI) blend membrane improved the CO_2/methane (CH_4) selectivity over pure PSF membrane.[7] The higher PEI concentration led to decrease in CO_2 and CH_4 permeability and increase in CO_2/CH_4 selectivity due to rigidity of PEI chains. Additionally, polymer concentration plays a critical role for membrane fabrication. According to Alavi et al., a lower polydimethylsiloxane (PDMS) concentration formed a thin selective skin layer of the PDMS membrane.[8] It resulted in higher CO_2, N_2 and CH_4 permeance as the CO_2 (3457.0 GPU), N_2 (145.2 GPU) and CH_4 (3457.2 GPU) gases were allowed to pass through the PDMS membrane. The higher CO_2/N_2 (23.8) and CO_2/CH_4 (8.2) selectivity was due to more CO_2 gases permeating through the PDMS membrane as compared to the N_2 and CH_4.[8]

The aim of the present work was to develop a CAB membrane by blending two different molecular weights of 70000 and 65000 in order to improve the CO_2/N_2 selectivity. Therefore, two molecular weights of CAB polymer were

chosen. Up to date, there has been no report on synthesising this CAB blend membrane by blending different ratios of the polar acetyl group of 28–31 wt% and 12–15 wt% for CAB molecular weights of 65000 and 70000, respectively. Besides, the effect of polymer concentration and solvent exchange drying time on the CAB membrane structure was evaluated in this study. Polymer concentration has a large impact on membrane morphology and membrane separation performance. It causes the formation of thicker membrane that decreases gas selectivity and gas permeance when the polymer concentration increases significantly. The separation performance of the CAB polymer blending membrane and the pure CAB membrane were compared by calculating the CO_2, and N_2 permeances and CO_2/N_2 selectivity.

2. EXPERIMENTAL

2.1 Materials

The CAB polymer of molecular weight 70000 with an acetyl group of 12–15 wt% and the CAB polymer of molecular weight 65000 with acetyl group of 28–31 wt% were purchased from Sigma-Aldrich (Malaysia). The chemical solutions used for membrane fabrication were chloroform, isopropyl alcohol (99.6%) and n-hexane (99.8%). These which were purchased from Merck (Malaysia).

2.2 Fabrication of CAB Membrane

The CAB membrane was fabricated using the wet-phase inversion method. The casting solution contained 4 wt% CAB (70000 and 65000) and 96 wt% chloroform. The solution was stirred for 24 h to ensure that the CAB polymer dissolved completely. Then, the dope solution was sonicated by ultrasonic degasser to remove the air bubbles in the solution. The dope solution was cast with membrane film of uniform thickness of 250 μm by using an automatic film applicator. The membrane film was then allowed 5 min solvent evaporation time to evaporate the remaining solvent. The membrane was then immersed into distilled water for 24 h to remove the excess solvent from the membrane. In order to maintain the membrane structure, the membrane film was immersed in isopropyl alcohol for 1 h to replace the water within the membrane. Subsequently, the membrane film was immersed in n-hexane for another 1 h as this solvent is less volatile and minimises the capillary force within the membrane. Thus, the membrane structure was maintained. The fabricated CAB membrane was placed between two glass plates filled with filter papers for 24 h to remove the remaining volatile liquid on the membrane film. The fabricated CAB membrane was stored before use.[9]

2.2.1   Effect of CAB polymer concentration of different molecular weights

The other CAB membrane was fabricated based on the membrane fabrication method. Different molecular weight contents of CAB polymer were used on CAB membrane as tabulated in Table 1.

Table 1: Preparation of CAB membrane at different content of molecular weight.

Sample description	CAB (wt%)	CAB (molecular weight 70000)	CAB (molecular weight 65000)	Casting thickness (μm)	Hexane exchange drying time (min)	Isopropyl alcohol exchange drying time (min)
M1	4	0.75	0.25	250	60	60
M2	4	0.6	0.4	250	60	60
M3	4	0.4	0.6	250	60	60
M4	4	0.3	0.7	250	60	60

2.3   Membrane Characterisation

2.3.1   SEM

The scanning electron microscope (SEM) was used to acquire visual information of membrane surface morphology and cross-sectional structure of the membrane. The membrane sample was cooled in the freezer at about –80°C for 24 h so that the membrane was easy to cut. The membrane sample was coated with a thin film of gold and platinum to improve the contrast and prevent the deterioration of image information.[10] The membrane thickness was determined by using the ImageJ software. Fewer results were collected for consistency.

2.3.2   ATR-FTIR spectroscopy

The attenuated total reflectance-Fourier transform infrared (ATR-FTIR) spectroscopy was used to analyse the functional group and bond of membrane. The range of ATR-FTIR was from 400 cm^{-1} to 4000 cm^{-1}. The radiation beam was absorbed by the sample and the reflected radiation beam was collected by the detector. The information for room condition was collected first to obtain the spectra wave number of samples.[11] Fewer results were again collected for consistency.

2.4 Membrane Separation Performance Test

The gas permeation test was performed to evaluate the separation performance of the CAB membrane. The gas permeation test was conducted based on previous published works.

$$\frac{P}{\ell} = \frac{Q}{A\Delta p} \tag{1}$$

$$\alpha_{CO_2}/N^2 = \frac{\left(\frac{p}{\ell}\right)_{CO_2}}{\left(\frac{p}{\ell}\right)_{N_2}} \tag{2}$$

where,

$\frac{P}{\ell}$ = gas permeance (GPU)

ℓ = membrane thickness (cm)

Q = volumetric flow rate (cm³ s⁻¹)

A = effective membrane area (cm³)

Δp = pressure difference across membrane (cmHg)

α = gas selectivity

2.5 Calculation of Average Acetyl Content of CAB Membranes

According to Sigma-Aldrich, the composition of CAB with molecular weight of 65000 is 29.5 wt% acetyl, 17.75 wt% butyryl and 1.1 wt% hydroxyl, while the composition of CAB with molecular weight of 70000 is 13.5 wt% acetyl, 37 wt% butyryl and 1.7 wt% hydroxyl. The average acetyl content of blend membrane, which was synthesised from two different ratios of molecular weights was calculated by using the following Equation 3:[12]

$$AAC = BR_{70000} \times AC_{70000} + BR_{65000} \times AC_{65000} \tag{3}$$

where AAC = average acetyl content (%), BR = blending ratio, and AC = acetyl content (%).

3. RESULTS AND DISCUSSION

3.1 Effect of CAB Polymer Concentration at Different Molecular Weights

The polymer blending at different molecular weights was one of the crucial factors that affected the morphology and gas separation performance of the membrane.[13] Therefore, CAB membrane was fabricated using different blend compositions to investigate the effect of polymer blending, which correlated with membrane structure. To have a better understanding on the behaviour of membrane gas transport, SEM analysis was conducted to observe the membrane surface and cross-sectional morphologies of the CAB membrane, which also controls the gas transport mechanism through the membrane. Figure 1 demonstrates the membrane surface and cross-sectional morphologies for the CAB membranes with molecular weights of 70000 and 65000 blended at different ratios of M1 (0.75:0.25), M2 (0.6:0.4), M3 (0.4:0.6) and M4 (0.3:0.7). Figure 1(a, c, e, g) shows the smooth and defect free surfaces for M1, M2, M3 and M4. This was due to bonding between the hydroxyl groups of the CAB polymer. The hydrogen bonding between the hydroxyl groups caused the polymer chains to become rigid, which restricted the formation of voids in the neighbouring C-OH rings, thus resulting in homogeneity on the surface of the membrane. This is shown in Figure 2.

Additionally, ATR-FTIR was used to investigate the intermolecular forces between the functional groups within the CAB membrane. The ATR-FTIR showed that the functional groups within CAB membrane improved the CO_2 solubility. The ATR-FTIR spectra for M1, M2, M3 and M4 are demonstrated in Figure 2. Based on the figure, the absorption band at around 2950 cm^{-1} was attributed to the stretching of the methyl (C-H) group.[14] Moreover, the band at around 1800 cm^{-1} was assigned to the carbonyl group vibration of carboxylic (C=O) group.[15] Furthermore, the band at 1395 cm^{-1} represented the hydroxyl (-OH) group and the band at around 1200 cm^{-1} was referred to as the stretching of the acrylate (C-O) group.[16] In addition, the band at 1030 cm^{-1} was assigned as the stretching of the ether (C-O-C) group.[17]

As seen in Figure 2, the polar functional groups in the CAB polymer that affected the gas separation performance were C=O group and O-H group.[18] The C=O and O-H groups had hydrogen bond interaction with CO_2 molecules.[19] Thus, the C=O and O-H groups interacted with the CO_2 gas and increased the CO_2 permeance and CO_2/N_2 selectivity. Based on Figure 2, M3 had higher absorption band of O-H, C=O, C-O and C-O-C groups. This was due to the increase in the content to 60% of the CAB with molecular weight of 65000 in the blend. Therefore, M3 contained more O-H, C=O, C-O and C-O-C groups, which when bonded with each other strengthened the intermolecular hydrogen bonding.[20]
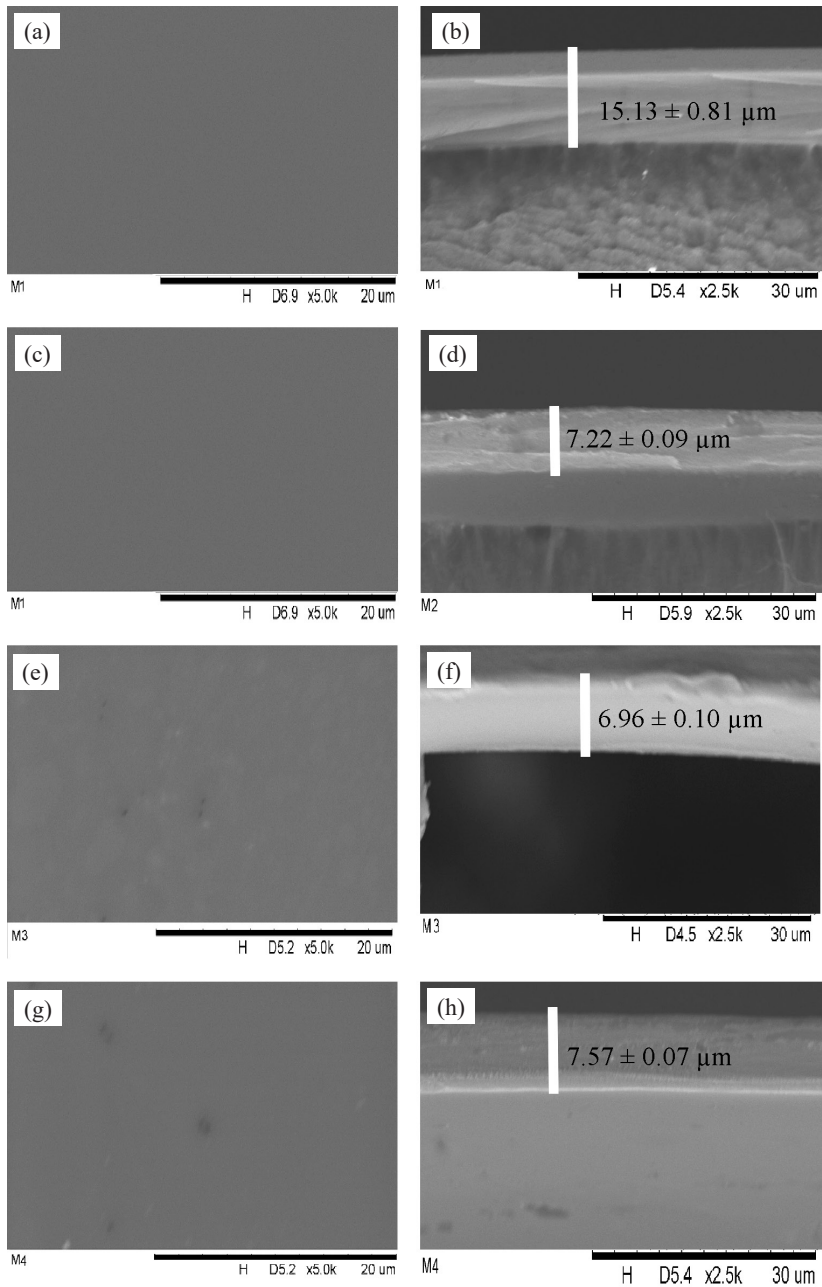
Figure 1:   SEM micrographs of surface (a, c, e, g) and cross section (b, d, f, h) for M1, M2, M3 and M4, 4 wt% CAB polymer concentration, 250 μm casting thickness, 5 min solvent evaporation time, 1 h isopropyl alcohol and 1 h hexane solvent exchange drying time.
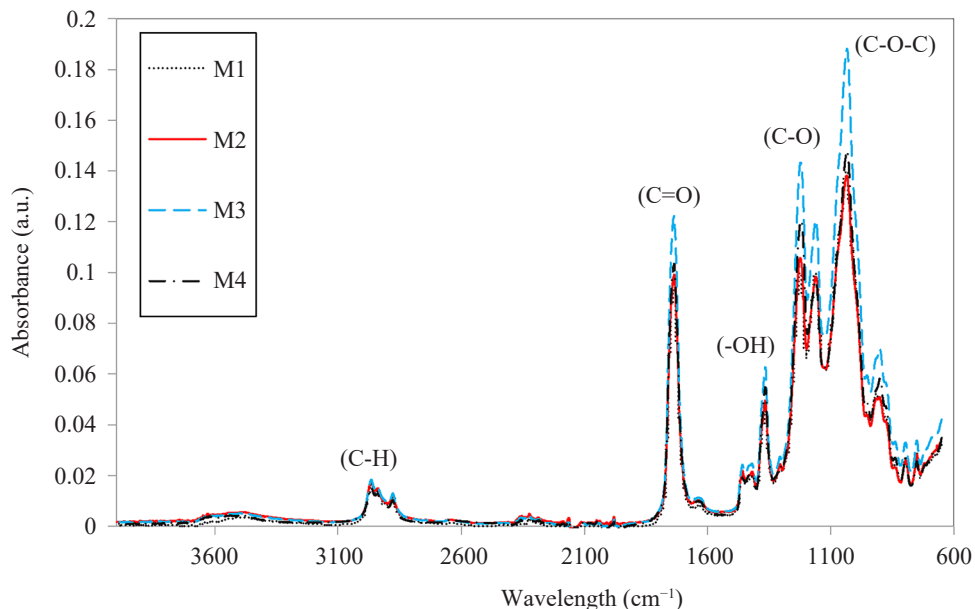
Figure 2:   ATR-FTIR for M1, M2, M3 and M4, 4 wt% CAB polymer concentration, 250 μm casting thickness, 5 min solvent evaporation time, 1 h isopropyl alcohol and 1 h hexane solvent exchange drying time.

Based on Figure 1(b, d, f, g), the membrane thickness reduced from 15.13 ± 0.81 μm for M1 to 6.96 ± 0.10 μm for M3. This was due to the increase in the CAB polymer concentration with molecular weight of 65000 from 0.25 to 0.6, which strengthened the thermodynamic instability of the dope solution. Moreover, the increment in the polymer concentration increased the solvent diffusivity, which caused more solvent to evaporate from the cast polymer solution resulting in reduced membrane thickness.[21] Besides that, the membrane thickness of M3 increased from 6.96 ± 0.10 μm to 7.57 ± 0.07 μm, as demonstrated in Figure 1(f and h). This was due to the strong interaction between solvent and polymer, which accelerated the aggregation of polymer molecules and formed a thicker membrane.[22]

Based on Figure 3, the CO_2 permeance decreased from 129.55 ± 0.58 GPU for M1 to 6.25 ± 0.08 GPU for M4. This observation was due to the increased acetyl content within the CAB membrane, as shown in Table 2. Therefore, the increase in the composition of CAB with molecular weight of 65000 increased the acetyl content within the CAB membrane, resulting in more acetyl groups bonding with each other. This caused the polymer chain to become more rigid, resulting in the reduction of the chain segment mobility of CAB.[23] Moreover, the low polymer

chain segment mobility of CAB membrane restricts the diffusion of CO_2 gas molecules.[24] Thus, the CO_2 gas molecules took a tortuous path to get through the CAB membrane.[25]

Table 2: Summary of calculated average acetyl content of CAB membrane at different ratios for molecular weights of 70000 and 65000.

Membrane	Ratio of molecular weight of 70000	Ratio of molecular weight of 65000	Calculated average acetyl content (wt%)
M1	0.75	0.25	17.5
M2	0.6	0.4	19.9
M3	0.4	0.6	23.1
M4	0.3	0.7	24.7

The increase in the CO_2 permeance of M1 was due to the membrane structure becoming less dense. This is demonstrated in Figure 1(b). In addition, the formation of the thicker and less dense membrane was due to the weak intermolecular force within the CAB membrane. As previously described in Figure 2, a possible explanation was that the absorbance band of O-H group for M1, which was prepared by blending the CAB polymer with molecular weights of 70000 and 65000 at ratio of 0.75:0.25, respectively, was at its lowest. Thus, having fewer O-H groups resulted in the formation a weak intermolecular force, which caused the polymer chain apart from each other.[26] Hence, it was proven that the flow resistance to the membrane decreased causing more CO_2 molecules to pass through the membrane.[27]

With reference to Figure 4, the nitrogen (N_2) permeance reduced significantly from 49.04 ± 0.61 GPU for M1 to 4.07 ± 0.02 GPU for M4. The reduction in N_2 permeance was due to the strong intermolecular hydrogen bonding within the CAB polymer matrix (Figure 2). Moreover, the strong intermolecular hydrogen bonding was formed by the increased interaction between O-H and C=O groups. Besides that, N_2 is a non-polar molecule and interacts less with hydrogen bonding in the CAB.[28] Thus, the N_2 gas has lower solubility than CO_2 in the polymer structure of CAB and shows lower gas permeances than CO_2.[29] The dramatic increment in the N_2 permeance of M1 was due to the weak intermolecular hydrogen bonding within the CAB membrane, as demonstrated in Figure 2. This result occurred because less O-H and C=O groups interacted with each other to form hydrogen bonding.[30] Therefore, the weak intermolecular hydrogen bonding reduced density, which led to an increase in chain flexibility and mobility in the CAB membrane. Thus, low packing chain density of the CAB membrane caused more N_2 gases to pass through the membrane, which increased the N_2 permeance.[31]
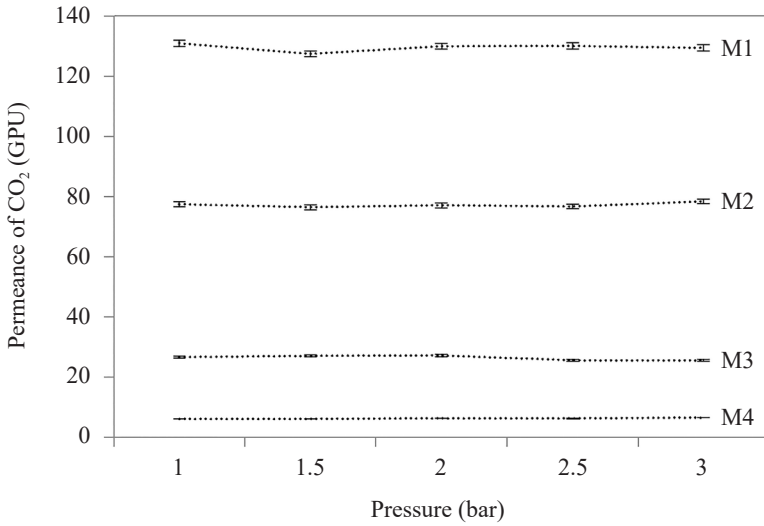
Figure 3: CO_2 permeance for M1, M2, M3 and M4, 4 wt% CAB polymer concentration, 250 μm casting thickness, 5 min solvent evaporation time, 1 h isopropyl alcohol and 1 h hexane solvent exchange drying time.
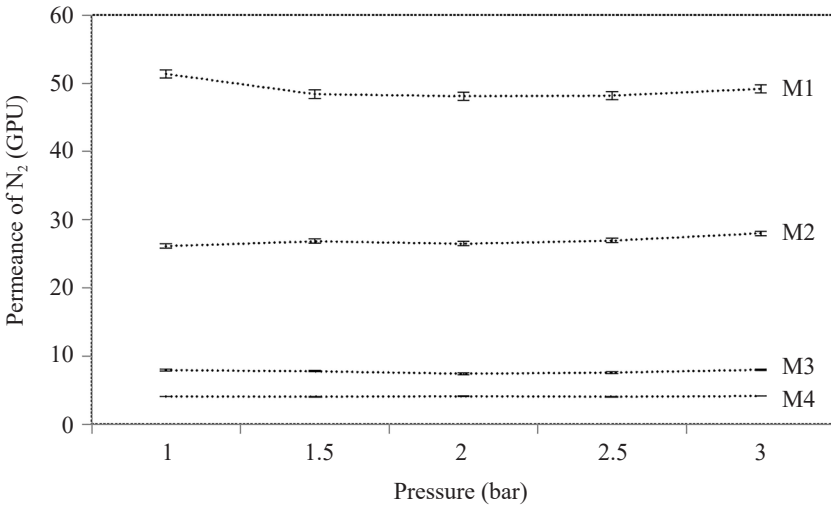

Figure 4: N_2 permeance for M1, M2, M3 and M4, 4 wt% CAB polymer concentration, 250 μm casting thickness, 5 min solvent evaporation time, 1 h isopropyl alcohol and 1 h hexane solvent exchange drying time.

Based on Figure 5, the CO_2/N_2 selectivity increased significantly from 2.64 ± 0.03 for M1 to 3.41 ± 0.08 for M3. The significant increase in CO_2/N_2 selectivity was due to the increase in the polar functional groups (C=O and O-H), which improved the polarity of the CAB membrane, resulting in favourable conditions for the CO_2 solubility.[32] Besides that, the absorbance bands of O-H and C=O groups for M3 were the highest, as demonstrated in Figure 2. M3 was prepared by blending the CAB polymer with molecular weights of 70000 and 65000 in the ratio of 0.4:0.6, respectively. Thus, with the help of strong intermolecular hydrogen bonding, the CO_2 solubility of M3 was enhanced. In addition, the CO_2 solubility was promoted because the CO_2 served as an electron acceptor and interacted with the polar functional groups in the CAB polymer.[33] This increased the interaction between the polar functional groups and CO_2, which caused high CO_2 affinity in the CAB polymer than for N_2.[34] Hence, both the O-H and C=O groups have strong attraction for CO_2, which increased the CO_2 permeance and improved the CO_2/N_2 selectivity. In addition, when the pressure increased from 2 bars to 3 bars, the CO_2/N_2 selectivity of M3 decreased slightly. This might be due to more N_2 gases passing through the membrane resulting in a slight increase in the N_2 permeance (Figure 4) and decrease in the CO_2/N_2 selectivity. However, the CO_2/N_2 selectivity decreased from 3.42 ± 0.08 (M3) to 1.54 ± 0.01 (M4). This result most likely occurred due to the structure of the dense membrane (7.57 ± 0.07 µm), as demonstrated in Figure 1(h). The formation of dense membrane was due to the strong interaction between solvent and polymer that decreased the dissolving capability of solvent for polymer. In addition, it caused the polymer molecules aggregation through chain entanglement and increased the membrane thickness.[35] Therefore, the dense membrane structure could have contributed to the reduced CO_2 and N_2 permeances and decreased CO_2/N_2 selectivity. Hence, the thicker dense CAB membrane restricted the diffusion of the CO_2 and N_2 gases.[36]

The effect of CAB polymer concentration at different molecular weights for separation of CO_2/N_2 is summarised in Figure 6. Based on the figure, the M3 membrane proved to have the highest CO_2/N_2 selectivity (3.41 ± 0.08) result amongst the others (M1, M2 and M4). Therefore, an increase in the content of CAB with molecular weight of 65000 caused the formation of a much thinner and denser membrane, which improved the separation performance. On the other hand, the M1 membrane had the highest CO_2 (129.55 ± 0.58 GPU) and N_2 permeances (49.04 ± 0.61 GPU). Hence, a low content of CAB with molecular weight of 65000 caused the membrane to become less dense, which led to more gas permeating through it. The effect of polymer concentration and blend composition affected the membrane morphology and membrane separation performance.
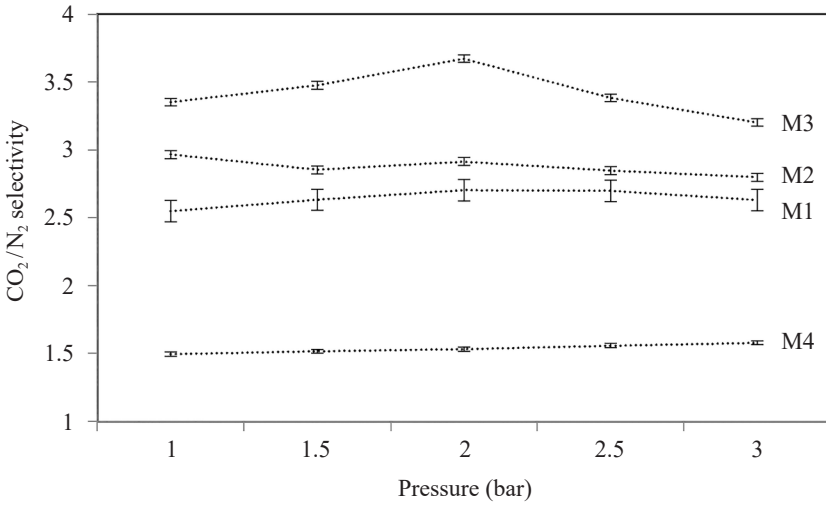
Figure 5: Ideal selectivity of CO_2/N_2 for M1, M2, M3 and M4, 4 wt% CAB polymer concentration, 250 μm casting thickness, 5 min solvent evaporation time, 1 h isopropyl alcohol and 1 h hexane solvent exchange drying time.

Figure 6: Summary of CO_2/N_2 permeation properties for M1, M2, M3 and M4, 4 wt% CAB polymer concentration, 250 μm casting thickness, 5 min solvent evaporation time, 1 h isopropyl alcohol and 1 h hexane solvent exchange drying time.
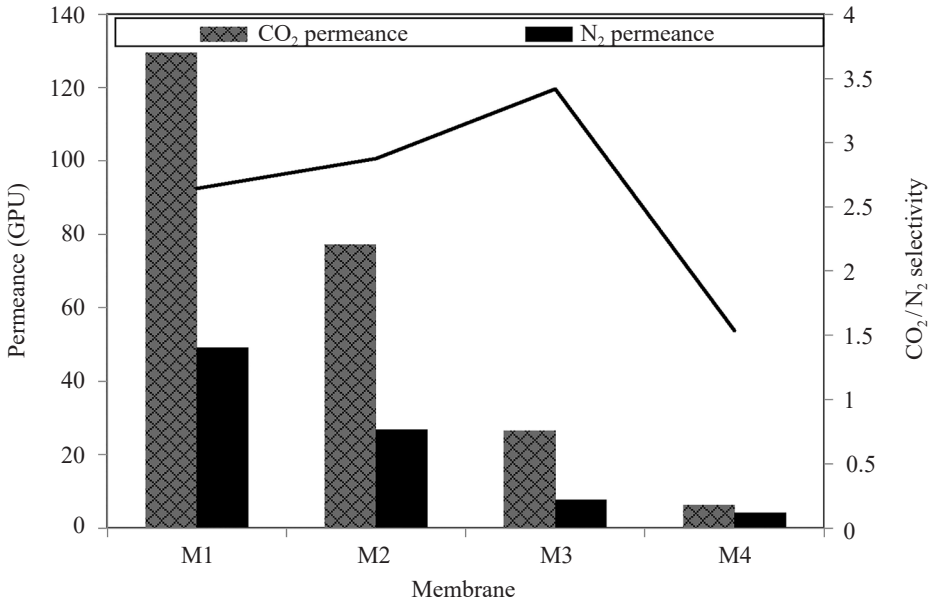
In conclusion, the present work was compared to other research works, which synthesised the CAB membrane with molecular weight of 70000, as summarised in Table 3. Based on gas separation performance, the M3 membrane obtained the highest CO_2/N_2 selectivity (3.42) in the present work as compared to Lee et al.[9] However, in comparison, M3 obtained lower CO_2 and N_2 permeances in this work. This was due to lower gas diffusivity of the denser membrane and therefore less CO_2 and N_2 gases diffused through the membrane.[37] These findings confirmed that the blending of CAB polymer at different molecular weights improved the membrane morphology and enhanced the CO_2/N_2 selectivity of the CAB membrane. In the future, it is expected that the permeance of CO_2 and N_2 performance of this newly CAB membrane will be further enhanced by embedding inorganic fillers within the membrane structure.

Table 3:　Summary of CO_2/N_2 permeation properties achieved from present work compared to other research study.

References	Polymer	Molecular weight 70000	Molecular weight 65000	P_{CO_2}	P_{N_2}	α_{CO_2/N_2}
Present work	CAB	0.4	0.6	26.39 GPU	7.730 GPU	3.42
Lee et al.[9]	CAB	1	0	120.19 GPU	37.91 GPU	3.17

4.　CONCLUSION

The CAB membrane was developed by blending two different molecular weights, i.e., 70000 and 65000. In this study, polymer concentration was investigated. Therefore, the membrane with molecular weights of 70000 and 65000 blended in the ratio of 0.4:0.6 resulted in the formation of a thinner dense membrane. Moreover, the thinner membrane showed the highest gas selectivity (3.42) due to the denser membrane structure and strong intermolecular hydrogen bonding, which improved the CO_2 solubility. The high gas permeance and high CO_2/N_2 selectivity was due to lower collapse of membrane structure. The results from this study showed that the CAB membrane with molecular weights of 70000 and 65000 blended in the ratio of 0.4:0.6, with 4 wt% of CAB polymer concentration had the best CO_2/N_2 separation performance.

5.   ACKNOWLEDGEMENTS

6.   REFERENCES

1.   Graven, H. et al. (2018). Assessing fossil fuel CO_2 emissions in California using atmospheric observations and models. *Environ. Res. Lett.*, 13(6), 065007. https://doi.org/10.1088/1748-9326/aabd43

2.   Ma, J., Ping, D. & Dong, X. (2017). Recent developments of graphene oxide-based membranes: A review. *Membr.*, 7(3), 1–29. https://doi.org/10.3390/membranes7030052

3.   Scholes, C. A., Stevens, G. W. & Kentish, S. E. (2012). Membrane gas separation applications in natural gas processing. *Fuel*, 96, 15–28. https://doi.org/10.1016/j.fuel.2011.12.074

4.   Han, G., de Wit, J. S. & Chung, T.-S. (2015). Water reclamation from emulsified oily wastewater via effective forward osmosis hollow fiber membranes under the PRO mode. *Water Res.*, 81, 54–63. https://doi.org/10.1016/j.watres.2015.05.048

5.   Seymour, R. W., Weinhold, S. & Haynes, S. K. (1979). Mechanical and dielectric relaxation in cellulose esters. *J. Macromol. Sci. B*, 16(3), 337–353. https://doi.org/10.1080/00222347908212300

6.   Park, H. et al. (2017). Maximizing the right stuff: The trade-off between membrane permeability and selectivity. *Sci.*, 356(6343), 1138–1148. https://doi.org/10.1126/science.aab0530

7.   Mukhtar, H. et al. (2016). Polymer blend membranes for CO_2 separation from natural gas. *IOP Conf. Ser. Earth Environ. Sci.*, 36(1), 012016. https://doi.org/10.1088/1755-1315/36/1/012016

8.   Alavi, S. et al. (2017). Preparation and characterization of PDMS/zeolite 4A/PAN mixed matrix thin film composite membrane for CO_2/N_2 and CO_2/CH_4 separations. *Res. Chem. Intermed.*, 43(5), 2959–2984. https://doi.org/10.1007/s11164-016-2806-2

9.   Lee, R. J. et al. (2017). Improvement of CO_2/N_2 separation performance by polymer matrix cellulose acetate butyrate. *IOP Conf. Ser. Mater. Sci. Eng.*, 206(1), 012072. https://doi.org/10.1088/1757-899X/206/1/012072

10.   Tylkowski, B. & Tsibranska, I. (2014). Overview of main techniques used for membrane characterization. *J. Chem. Technol. Metal.*, 50(1), 3–12.

11.   Barbes, L., Radulescu, C. & Stihi, C. (2014). ATR-FTIR spectrometry characterisation of polymeric materials. *Rom. Rep. Phys.*, 66(3), 765–777.

12.   Ferraz, A. et al. (2000). Estimating the chemical composition of biodegraded pine and eucalyptus wood by DRIFT spectroscopy and multivariate analysis. *Bioresour. Technol.*, 74(3), 201–212. https://doi.org/10.1016/S0960-8524(00)00024-9

13.   Mushtaq, A., Mukhtar, H. & Shariff, A. M. (2013). Blending behavior of polysulfone, polyvinyl acetate and amines in dimethyl acetamide solvent. *J. Sci. Eng. Technol.*, 7(8), 1634–1641.

14.   Lavorgna, M. et al. (2012). Silanization and silica enrichment of multiwalled carbon nanotubes: Synergistic effects on the thermal-mechanical properties of epoxy nanocomposites. *Eur. Polym. J.*, 49(2), 428–438. https://doi.org/10.1016/j.eurpolymj.2012.10.003

15.   Suttiwijitpukdee, N. et al. (2011). Intermolecular interactions and crystallization behaviors of biodegradable polymer blends between poly (3-hydroxybutyrate) and cellulose acetate butyrate studied by DSC, FT-IR, and WAXD. *Polym.*, 52(2), 461–471. https://doi.org/10.1016/j.polymer.2010.11.021

16.   Del Valle, E. M. M. (2004). Cyclodextrins and their uses: A review. *Process Biochem.*, 39(9), 1033–1046. https://doi.org/10.1016/S0032-9592(03)00258-9

17.   Lou, Y. et al. (2014). A facile way to prepare ceramic-supported graphene oxide composite membrane via silane-graft modification. *Appl. Surf. Sci.*, 307, 631–637. https://doi.org/10.1016/j.apsusc.2014.04.088

18.   Shan, M. et al. (2012). Influence of chemical functionalization on the CO_2/N_2 separation performance of porous graphene membranes. *Nanosc.*, 4(17), 5477–5482. https://doi.org/10.1039/c2nr31402a

19.   Xing, W. et al. (2014). Oxygen-containing functional group-facilitated CO_2 capture by carbide-derived carbons. *Nanosc. Res. Lett.*, 9(1), 1–8. https://doi.org/10.1186/1556-276X-9-189

20.   El-Sakhawy, M. et al. (2018). Preparation and infrared study of cellulose based amphiphilic materials. *Cell. Chem. Technol.*, 52(3–4), 193–200.

21.   Ikhsan, D. et al. (2017). Effect of combination dope composition and evaporation time on the separation performance of cellulose acetate membrane for demak brackish water treatment. *MATEC Web Conf.*, 101, 01004. https://doi.org/10.1051/matecconf/201710101004

22.   Mustaffar, Ismail, A. & Illias, R. (2018). Study on the effect of polymer concentration on hollow fiber ultrafiltration membrane performance and morphology. Unpublished paper, Faculty of Chemical and Natural Engineering, Universiti Teknologi Malaysia, 1–12.

23.   Marais, S. et al. (2004). Transport of water and gases through EVA/PVC blend films—permeation and DSC investigations. *Polym. Test.*, 23(4), 475–486. https://doi.org/10.1016/j.polymertesting.2003.09.009

24.   Zhang, H. & Cloud, A. (2006). The permeability characteristics of silicone rubber. Unpublished technical paper, Arlon Silicone Technologies Division, Delaware.

25.   Liu, Y. et al. (2014). Enhanced CO_2 permeability of membranes by incorporating polyzwitterion@CNT composite particles into polyimide matrix. *ACS Appl. Mater. Interf.*, 6(15), 13051–13060. https://doi.org/10.1021/am502936x

26. Krishnamurthi, P.P., Ramalingam, H. B. & Raju, K. P. (2015). FTIR studies of hydrogen bonding interaction between the hydroxyl and carbonyl liquids. *Adv. Appl. Sci. Res.*, 6(12), 44–52.

27. Ngogu, N. & Gobina, E. (2015). Gas permeation behavior of single and mixed gas components using an asymmetric ceramic membrane. *Int. J. Mater. Metal. Eng.*, 9(6), 689–693. https://doi.org/10.5281/zenodo.1107233

28. Marsh, K. N., Boxall, J. A. & Lichtenthaler, R. (2004). Room temperature ionic liquids and their mixtures—A review. *Fluid Phase Equilib.*, 219(1), 93–98. https://doi.org/10.1016/j.fluid.2004.02.003

29. Lee, R. J. et al. (2018). Incorporation of functionalized multi-walled carbon nanotubes (MWCNTs) into cellulose acetate butyrate (CAB) polymeric matrix to improve the CO_2/N_2 separation. *Process. Saf. Environ.*, 117, 159–167. https://doi.org/10.1016/j.psep.2018.04.021

30. Powell, C. E. & Qiao, G. G. (2006). Polymeric CO_2/N_2 gas separation membranes for the capture of carbon dioxide from power plant flue gases. *J. Membr. Sci.*, 279 (1), 1–49. https://doi.org/10.1016/j.memsci.2005.12.062

31. Jie, X. et al. (2004). Gas permeation performance of cellulose hollow fiber membranes made from the cellulose/N-methylmorpholine-N-oxide/H_2O system. *J. Appl. Polym. Sci.*, 91(3), 1873–1880. https://doi.org/10.1002/app.2385

32. Mazinani, S. et al. (2018). A ground breaking polymer blend for CO_2/N_2 separation. *J. CO_2 Utiliz.*, 27, 536–546. https://doi.org/10.1016/j.jcou.2018.08.024

33. Yuan, Y. & Teja, A. S. (2011). Quantification of specific interactions between CO_2 and the carbonyl group in polymers via ATR-FTIR measurements. *J. Superc. Fluids*, 56(2), 208–212. https://doi.org/10.1016/j.supflu.2010.12.010

34. Kunthadong, P. et al. (2015). Biodegradable plasticized blends of poly(l-lactide) and cellulose acetate butyrate: From blend preparation to biodegradability in real composting conditions. *J. Polym. Environ.*, 23(1), 107–113. https://doi.org/10.1007/s10924-014-0671-x

35. Kimmerle, K. & Strathmann, H. (1990). Analysis of the structure-determining process of phase inversion membranes. *Desalin.*, 79(2–3), 283–302. https://doi.org/10.1016/0011-9164(90)85012-y

36. Tan, P. C. et al. (2016). Correlation between polymer packing and gas transport properties for CO_2/N_2 separation in glassy fluorinated polyimide membrane. *J. Eng. Sci. Technol. Rev.*, 11(7), 935–946.

37. Fu, Y. et al. (2018). Ultra-thin enzymatic liquid membrane for CO separation and capture. *Nat. Comm.*, 9(1), 990–990. https://doi.org/10.1038/s41467-018-03285-x